ON THE METALLICITY AND THE TURNOFF AGE OF NGC 188

L. M. Hobbs[a] and J. A. Thorburn
Yerkes Observatory, University of Chicago, Williams Bay, Wisconsin 53191-0258

Theodore Rodriguez-Bell
Astronomy and Astrophysics Center, University of Chicago, 5640 S. Ellis Avenue, Chicago, Illinois 60637
Received 26 March 1990; revised 24 May 1990

ABSTRACT

High-dispersion echelle spectra of seven stars located within the turnoff region in NGC 188 are analyzed, using the model atmospheres of Kurucz. An average iron abundance of the cluster, relative to the Sun, of [Fe/H] $= -0.12 \pm 0.16$ is derived from the observed equivalent widths of up to six weak Fe II lines in each of the seven spectra and in the solar spectrum. With this known relative iron abundance, the equivalent widths of up to eight weak Fe I lines in these same spectra then require that the effective temperatures of the turnoff stars average $\langle T_e \rangle_{\rm turnoff} = 5885 \pm 120$ K. The uncertain Fe II oscillator strengths were calibrated by requiring that, for the physically very similar Sun, the identical analysis recover the correct effective temperature from the same Fe II and Fe I lines. Finally, a turnoff age of $\tau = 7.7 \pm 1.4$ Gyr is derived by comparing the deduced upper limit on these turnoff temperatures to appropriate isochrones in the theoretical H–R diagram, as calculated anew by VandenBerg (1990). A primary advantage of this purely spectroscopic method is that it effectively requires no estimates of the reddening or the intrinsic colors of the cluster stars or of the distance to the cluster; the attendant uncertainties in these cluster parameters are thereby circumvented entirely. A similar, auxiliary investigation of the luminosities of the cluster stars in the H–R diagram favors the young end of the cited range of ages, but it is less intrinsically reliable owing to its sensitivity to possible errors in the assumed cluster parameters.

I. INTRODUCTION

As the nearest, best-studied example of the oldest open clusters, NGC 188 is of noteworthy importance in the study of Galactic evolution. Reliable determinations specifically of the age and the metallicity of the cluster are vital in investigations of such diverse questions as, for example, the formation of the disk (Larson 1990), the rate of production of the heavy elements (Wheeler, Sneden, and Truran 1989), and primordial nucleosynthesis (Hobbs and Pilachowski 1988). Quantitative estimates of the age and the average metallicity of the stars in NGC 188 have been almost exclusively derived photometrically, from the colors of the rather faint cluster members. Using the difference in the effects caused in the $(U-B)$, $(B-V)$ color–color diagram by changes in the heavy-element abundances relative to the Hyades and in the reddening, respectively, Eggen and Sandage (1969; hereafter referred to as ES) determined both cluster parameters separately, concluding that [Fe/H]≈ 0 and $E(B-V) = 0.09$. On the other hand, it has long been realized that, in general, quite small errors in any estimate of the cluster's reddening can cause significant errors in the derived values of the age and the metallicity (e.g., Twarog and Anthony-Twarog 1989).

High-dispersion echelle spectra of six main-sequence, proper-motion members of the cluster which are found in the turnoff region have been obtained previously at Kitt Peak National Observatory, primarily to measure the Li I λ 6707 line (Hobbs and Pilachowski 1988). A similar spectrum was also obtained of a seventh, apparent main-sequence member of the cluster which is too faint to have been included in the proper-motion survey of Upgren, Mesrobian, and Kerridge (1972). This star, I-49, will also be assumed to be a cluster member, since its radial velocity measured in our spectra is consistent with cluster membership. Most of our spectra of these stars fully cover the wavelength range from about 5100 to 6900 Å; considerable gaps exist in this spectral coverage in a few exposures obtained with a different camera on the spectrograph. The spectra therefore include a number of weak Fe II lines which can give direct, reliable determinations of the cluster's iron abundance which are nearly unaffected by the actual uncertainties in the effective temperatures of the relevant cluster stars; the importance of using the Fe II lines, not the Fe I lines, has been emphasized by Blackwell, Shallis, and Simmons (1980; hereafter referred to as BSS). Our first purpose is to report such a spectroscopically determined average value of [Fe/H] for NGC 188, which will in fact agree closely with the conclusion reached by ES two decades ago. In contrast to the Fe II lines, the strengths of the numerous weak lines of Fe I which are also present in the same spectra are known to depend very sensitively upon temperature. Once the abundance of iron has been previously deduced from the Fe II absorption, the lines of Fe I can therefore be used to estimate the effective temperatures of the stars. Our second purpose is to report such spectroscopically determined values of T_e in NGC 188. Finally, given this knowledge of the metallicity and the effective temperatures of stars near the main-sequence turnoff, any appropriate set of evolutionary stellar models can be used to obtain an estimate of the cluster's turnoff age as well, from the maximum stellar temperatures reached in the turnoff region.

A primary advantage of this purely spectroscopic method

[a] Visiting Astronomer, Kitt Peak National Observatory, National Optical Astronomy Observatories, operated by the Association of Universities for Research in Astronomy Inc. under contract with the National Science Foundation.

of determining values of [Fe/H], T_e, and age is its independence from uncertainties in the reddening and the distance of the cluster. A different set of potential errors is of course introduced, viz., those arising from any deficiencies in the Kurucz (1979) model atmospheres which are used to establish the iron abundance and the effective temperatures. Because the atmospheres of the main-sequence turnoff stars in NGC 188 appear to be physically very similar to that of the Sun, and because most solar equivalent widths are reproduced acceptably by Kurucz's solar model, the model atmospheres which are actually used in our differential analysis with respect to the Sun appear to be adequate for our purpose.

II. Fe II OSCILLATOR STRENGTHS

Very accurate transition probabilities are not yet available for the weak Fe II lines which are to be analyzed. This difficulty is not a serious impediment, because our primary interest lies in the iron abundance of the stars in NGC 188 relative to the Sun, rather than in either of the absolute abundances. In order to determine suitable, approximate Fe II oscillator strengths for this work, the analysis used for the cluster stars will also be required to give the correct results when applied to the Sun. This procedure is very similar to the method discussed and used by BSS, which is repeated only because we are using a different set of model atmospheres and slightly different solar equivalent widths. Briefly, since very accurate experimental oscillator strengths have been measured for the eight Fe I lines to be analyzed in the spectra of the cluster stars, the solar equivalent widths of those same lines can be used to determine an average absolute solar iron abundance, $\langle \mathrm{Fe/H} \rangle_\odot$. The oscillator strength of each of six Fe II lines to be analyzed in the spectra of the cluster stars can then be adjusted to give the same abundance, $\langle \mathrm{Fe/H} \rangle_\odot$, from the measured solar strength of that line.

The results of this analysis are collected in Table I, where the solar equivalent widths measured in integrated light by Rutten and van der Zalm (1984) are used, if available. For four lines not measured by those authors, we have determined values anew from the solar flux atlas of Kurucz *et al.* (1984). If a microturbulent velocity of 0.9 km s^{-1} is used in Kurucz's (1979) solar model ($T_e = 5770$ K, $\log g = 4.44$), the average of the individual iron abundances inferred from the eight solar Fe I lines is $\log \langle \mathrm{Fe/H} \rangle_\odot = -4.53 \pm 0.07$. This result is in good agreement with the value $\log \mathrm{Fe/H} = -4.50$ used by Kurucz (1979) in constructing the solar model. The resulting oscillator strengths then derived for each of the individual Fe II lines from this abundance, $\log \langle \mathrm{Fe/H} \rangle_\odot = -4.53$, are also listed in the table. The average excess of these six values over the corresponding results similarly obtained by BSS is $\Delta(\log gf) = +0.15 \pm 0.05$, a difference in fact equal to the typical uncertainty of ± 0.15 estimated by BSS for their own solar values of log *gf*. The oscillator strengths of Table I will therefore be adopted throughout this paper, which utilizes the Kurucz model atmospheres.

III. DATA AND RESULTS

a) The Spectra

The spectra of seven dwarfs and one subgiant in NGC 188 have been described by Hobbs and Pilachowski (1988); the region from about 6695 to 6725 Å in each of the spectra was also illustrated. The instrumental resolution of the observations was 0.2 Å, and a signal-to-noise ratio $S/N \approx 45$ typically was achieved, after the multiple exposures (usually two) of a given star were averaged together. The 2σ detection limit in the final spectra consequently is near an equivalent width $W_\lambda = 9$ mÅ. Independent measurements of the various lines studied in each of two or three similar exposures show empirically that, for any given line, the uncertainty in the equivalent width measured in our spectra is well approximated by this limit.

The equivalent widths of the Fe II and Fe I lines depend in general upon the star's iron abundance (and correlated overall metallicity), effective temperature, surface gravity, and atmospheric microturbulent velocity. For lines with $W_\lambda \lesssim 50$ mÅ, the dependence upon the unknown microturbulent velocity is rather weak. Our analysis in this paper is therefore largely confined to such weak lines, and a value $v_t = 1$ km s^{-1} is everywhere assumed for the cluster stars, for definiteness. On the other hand, the primary disadvantage of analyzing weak lines is that the precision attained in measuring the equivalent width of an individual line is usually poorer than about 20%, in view of the measurement errors cited above. However, the combination of the results ob-

TABLE I. The Fe I and Fe II lines utilized.

Ion	λ (Å)	Multiplet number	ΔE (ev)	log *gf*	Ref.[a]	$W_{\lambda,\odot}$ (mÅ)	Ref.[a]	log (Fe/H)$_\odot$
Fe I	6082.72	64	2.223	−3.573	1	33.6	3	−4.60
	6151.62	62	2.176	−3.299	1	50.8	4	−4.54
	6173.34	62	2.223	−2.880	1	73.9	4	−4.40
	6265.14	62	2.176	−2.550	1	89.1	4	−4.48
	6297.80	62	2.223	−2.740	1	73.8	3	−4.56
	6481.88	109	2.279	−2.984	1	63.1	4	−4.51
	6498.94	13	0.958	−4.687	2	43.9	4	−4.57
	6574.24	13	0.990	−5.004	2	26.6	3	−4.61
Fe II	5991.38	46	3.14	−3.64	3	29.1	4	−4.53
	6149.25	74	3.87	−2.76	3	36.3	4	−4.53
	6247.56	74	3.87	−2.31	3	55.1	3	−4.53
	6416.92	74	3.87	−2.68	3	39.8	4	−4.53
	6432.68	40	2.88	−3.65	3	39.6	4	−4.53
	6456.39	74	3.89	−2.10	3	64.1	4	−4.53

[a] References: 1 = Blackwell, Petford, Shallis, and Simmons (1982); 2 = Blackwell, Booth, Haddock, Petford, and Leggett (1986); 3 = this work; and 4 = Rutten and van der Zalm (1984).

tained, for example, from up to six Fe II lines in each of the seven program stars will yield a final average value of [Fe/H] which exhibits useful precision.

b) The Fe II Lines

Figure 1 shows the extremely weak temperature dependence of the Fe II λ 6247 line which is predicted theoretically from the model atmospheres. A typical uncertainty in T_e for the stars observed is ± 250 K (Sec. III*c*), which almost negligibly affects the observable equivalent widths in the spectra of our program stars. The strength of the λ 6247 line therefore primarily indicates a program star's iron abundance, which is the datum to be determined, and, to a lesser extent, its surface gravity. The other Fe II lines measured in this work show similar behavior.

A star's surface gravity can be calculated from the expression $g = 4\pi G \times \sigma T_e^4 \times (\mathscr{M}/L)$, where $L/\mathscr{M}$ is the ratio of the luminosity to the mass of the star. Especially when applied to isolated field stars which are highly evolved, this method can be affected by large uncertainties (Trimble and Bell 1981). For our program stars, however, all of which are located within a small region near the main sequence of the color–magnitude diagram of a well-studied cluster, this method provides adequately precise values of g, because it requires a knowledge only of T_e and the ratio $L/\mathscr{M}$. *For this immediate purpose only*, we adopt both the cluster distance modulus $m_0 - M = 10.85$ and the color excess $E(B-V) = 0.09$ found by ES, along with a representative mass $\mathscr{M}/\mathscr{M}_\odot = 1.0$ and temperature $T_e = 5950$ K, and the corresponding bolometric correction BC $= -0.05$ mag (Code *et al.* 1976). The choices of $\mathscr{M}$ and T_e are derived from our later results below. Table II gives the values of M_{bol}, $L/\mathscr{M}$, and log g calculated from the observed V magnitudes in this way. The values of log g derived for these solarlike stars are quite plausible, ranging from 4.38 for the star nearest the ZAMS to about 4.1 for the six brighter, more evolved stars. The latter results indeed agree quite well with the values log $g \approx 4.2$ predicted theoretically for turnoff stars along the isochrones of VandenBerg (1985), almost independently of age, in the range from 5 to 10 Gyr. The largest contribution to the uncertainty in the inferred surface gravities may arise from the corresponding uncertainty in the cluster's distance. The *ratio* of the values of g for any two stars, which is independent of both the distance and the reddening assumed, is probably uncertain by only $\pm 20\%$, or even less; the absolute value of g for any star may perhaps be in error by up to $\pm 45\%$. This accuracy is quite acceptable for our purpose, as can be seen from Fig. 1. It should also be noted that, for the six of our program stars which are common to both studies, the recent CCD photometry of Caputo *et al.* (1990) agrees, within the errors, with the older photoelectric data of ES. Specifically, in the sense of Caputo *et al.* minus ES, $\Delta(B-V) = -0.007 \pm 0.025$ and $\Delta V = +0.020 \pm 0.057$ for these six stars.

For each of seven stars in NGC 188, the observed equivalent widths of up to six Fe II lines previously enumerated in Table I are given in Table III; the region near the λ 6247 line in the various spectra is also illustrated in Fig. 2. No additional weak, unblended Fe II lines with oscillator strengths determined by BSS (as an independent check on our own) are detected reliably in our spectra of all seven stars. Most of the cases for which no entry is found in Table III were strongly affected by cosmic-ray impacts on the CCD detector. The equivalent widths of the Fe II lines measured in the integrated light of the Sun are also copied from Table I, and the essence of the final result of this section can now be anticipated immediately. In the spectrum of any star with a solar abundance of iron, but with a slightly higher effective temperature and a slightly lower surface gravity than the Sun, Fig. 1 shows that the observed Fe II lines should be slightly stronger than their respective solar counterparts, by

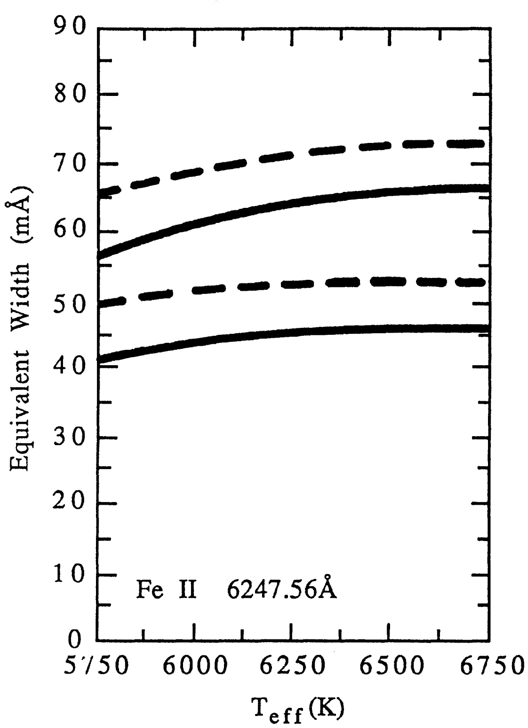

FIG. 1. The variation of the equivalent width of the 6247.56 Å line of Fe II with stellar effective temperature, as predicted by the Kurucz (1979) model atmospheres. The iron abundances assumed in deriving the upper and lower pairs of curves are log (Fe/H) $= -4.5$ and -5.0 respectively. The surface gravities assumed in deriving the dashed and the solid curves are log $g = 4.0$ and 4.5, respectively. A microturbulent velocity $v_t = 1$ km s^{-1} was used in all cases.

TABLE II. Surface gravities.

Star	V_0[a]	M_{bol}[b]	$(L/L_\odot)/(\mathscr{M}/\mathscr{M}_\odot)$[c]	log g[d]
I-91	14.56	3.66	2.75	4.05
I-76	14.66	3.76	2.51	4.09
I-99	14.66	3.76	2.51	4.09
I-17	14.71	3.81	2.40	4.11
I-101	14.72	3.82	2.38	4.12
I-71	14.81	3.91	2.19	4.15
I-49	15.37	4.47	1.31	4.38

Notes to TABLE II

[a] With $A_V = 3.1 \times E(B-V) = 0.28$ mag (ES).
[b] With $m_0 - M = 10.85$ mag (ES) and $BC = M_{bol} - M_V = -0.05$ (Code *et al.* 1976).
[c] With $\mathscr{M}/\mathscr{M}_\odot = 1.00$.
[d] With $T_e = 5950$ K.

TABLE III. Fe II lines.

Star	5991.38 Å W_λ (mÅ)	5991.38 Å log Fe/H	6149.25 Å W_λ (mÅ)	6149.25 Å log Fe/H	6247.56 Å W_λ (mÅ)	6247.56 Å log Fe/H	6416.92 Å W_λ (mÅ)	6416.92 Å log Fe/H	6432.68 Å W_λ (mÅ)	6432.68 Å log Fe/H	6456.39 Å W_λ (mÅ)	6456.39 Å log Fe/H	log $(\mathrm{Fe/H})_{\mathrm{star}}$	$[(\mathrm{Fe/H})]_{\mathrm{star}}$
I-91	31	−4.69	52	−4.32	73	−4.28	×	×	42	−4.65	79	−4.37	−4.43 ± 0.19	+0.10 ± 0.19
I-76	33	−4.67	39	−4.72	43	−5.09	32	−4.98	25	−5.13	58	−4.93	−4.88 ± 0.21	−0.35 ± 0.21
I-99	27	−4.79	50	−4.43	61	−4.58	33	−4.92	39	−4.72	69	−4.62	−4.65 ± 0.19	−0.12 ± 0.19
I-17	26	−4.79	45	−4.46	×	×	44	−4.59	50	−4.45	58	−4.80	−4.59 ± 0.17	−0.06 ± 0.17
I-101	30	−4.73	32	−4.89	60	−4.64	×	×	×	×	57	−4.91	−4.78 ± 0.14	−0.25 ± 0.14
I-71	×	×	35	−4.79	50	−4.87	22	−5.22	54	−4.39	72	−4.59	−4.69 ± 0.34	−0.16 ± 0.34
I-49	24	−4.79	44	−4.50	58	−4.61	×	×	×	×	52	−4.96	−4.68 ± 0.21	−0.15 ± 0.21
Sun	29.1	−4.53	36.3	−4.53	55.1	−4.53	39.8	−4.53	39.6	−4.53	64.1	−4.53	−4.53 ± 0.00	—

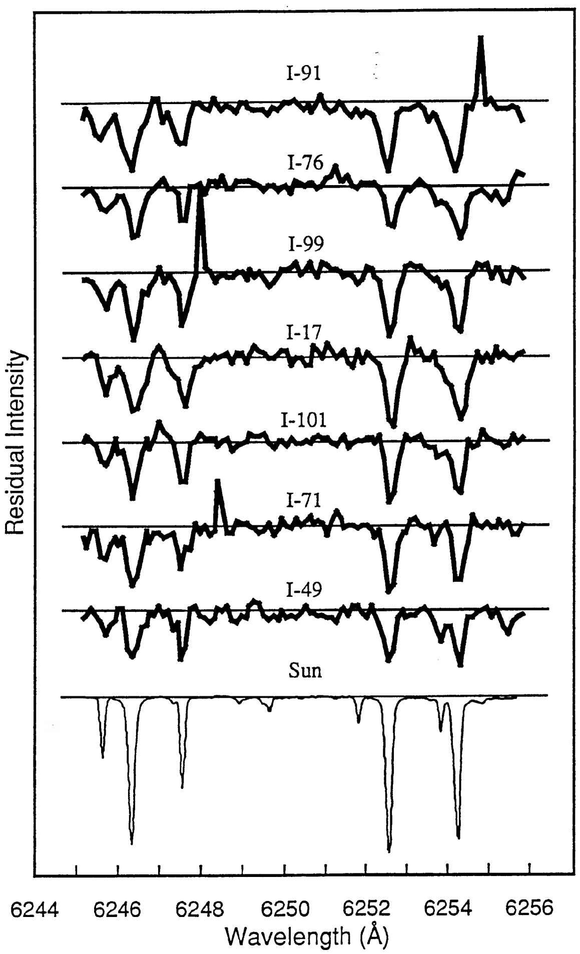

FIG. 2. The region near the 6247.56 Å line of Fe II in the spectra of the Sun and of seven stars found near the main-sequence turnoff in NGC 188. The continuum level of any spectrum corresponds to a residual intensity of 0.6 with respect to the adjacent spectrum above, and the resolution of the solar spectrum is better than that of the cluster spectra by a factor near 20. The three lines stronger than Fe II λ 6247.56 are Fe I λ 6246.33, Fe I λ 6252.57, and a blend of Si I λ 6254.17 and Fe I λ 6254.25. Two well-defined weaker lines are Sc II λ 6245.62 and Fe I λ 6253.83. The three conspicuous upward spikes result from the impacts of cosmic rays.

an amount which is to be compared to the present observational uncertainty $\Delta W_\lambda\,(2\sigma) \approx \pm 9$ mÅ. Any larger, detectable difference between the measured equivalent widths must therefore reveal a corresponding, real difference in Fe/H (or surface gravity) between the star in question and the Sun. The average ratio of the 35 equivalent widths reported in Table III for the cluster stars, relative to their solar counterparts, is 1.02 ± 0.21, in fact. The iron abundance in NGC 188 therefore must be about solar, or perhaps slightly lower, since the turnoff stars do indeed have slightly higher temperatures and lower gravities than the Sun.

The quantitative iron abundances, log Fe/H, given in Table III have been derived from the respective equivalent widths in combination with theoretical curves of growth W_λ (Fe/H; g, T_e). Similarly given is the overall iron abundance, $\log(\mathrm{Fe/H})_{\mathrm{star}}$, obtained for each star by averaging the individual results derived from the various lines. The curves of growth employed were calculated using the Kurucz (1979) model atmospheres and the WIDTH program; the stellar effective temperatures assumed while using the curves of growth were the final values to be described below (Sec. III*c*), while the gravities were those given in Table II.

For any single star, the standard deviation of the iron abundances deduced from the respective lines is $\sigma_{\log(\mathrm{Fe/H})} \approx 0.20$ (Table III). The random errors expected in the measured equivalent widths and in the oscillator strengths can account rather well for this dispersion. In addition, the largest difference in $\log(\mathrm{Fe/H})_{\mathrm{star}}$ between any two of our stars is 0.45, or about $2.2\sigma_{\log(\mathrm{Fe/H})}$, and five of the seven stellar abundances lie within the narrow range $-4.78 \leqslant \log(\mathrm{Fe/H})_{\mathrm{star}} \leqslant -4.59$. These results suggest that the apparent differences in iron abundance from star to star are random errors which do not exceed the expected uncertainties. Therefore, a more precise approximation to the average iron abundance in NGC 188 can be obtained by further averaging the respective iron abundances for all seven stars. The average value is $\log(\mathrm{Fe/H})_{\mathrm{cluster}} = -4.65 \pm 0.16$.

By precisely the same method, each of the solar equivalent widths necessarily gives $\log(\mathrm{Fe/H})_\odot = -4.53$ (Table III), because the values of the oscillator strengths in Table I were explicitly adjusted to yield this value. Owing to the absence of accurate, independent, experimental values of these Fe II oscillator strengths, the absolute iron abundances deduced for both the Sun and the cluster stars may be in error. A more accurately determined quantity therefore is

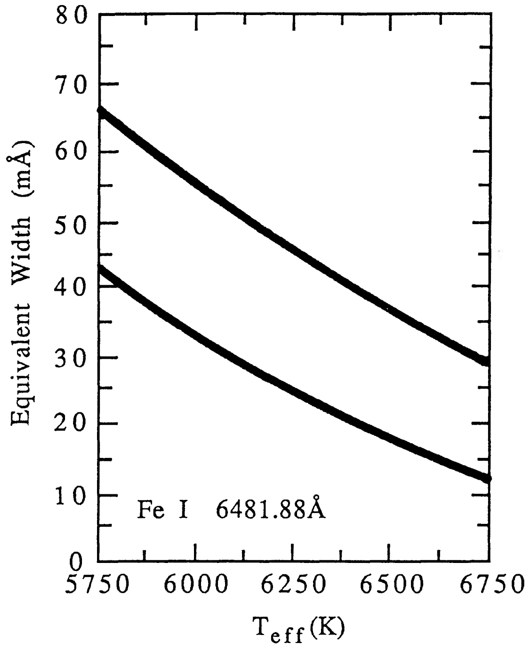

FIG. 3. The variation of the equivalent width of the 6481.88 Å line of Fe I with stellar effective temperature, as predicted by the Kurucz (1979) model atmospheres. The iron abundances assumed in calculating the upper and lower curves are log (Fe/H) = − 4.5 and − 5.0 respectively. For each of these abundances, the two curves representing the surface gravities log $g = 4.0$ and 4.5 effectively coincide (cf. Fig. 1). A microturbulent velocity $v_t = 1$ km s^{-1} was used in all cases.

the ratio of these abundances, which should be nearly independent of errors in the oscillator strengths. The iron abundances of the various cluster stars relative to the Sun, $[Fe/H]_{star} = \log[(Fe/H)_{star}/(Fe/H)_\odot]$, are given in the last column of Table III. For NGC 188, we therefore finally conclude that $[Fe/H]_{cluster} = \log[(Fe/H)_{cluster}/(Fe/H)_\odot] = -0.12 \pm 0.16$, in accordance with the qualitative conclusion previously inferred directly from the equivalent widths alone.

c) The Fe I Lines

Figure 3 shows the substantially more sensitive temperature dependence of the Fe I λ 6481 line which is predicted theoretically from the model atmospheres. Also illustrated is the effective invariance of this line's strength under changes in surface gravity, within the relevant range $4.0 \leqslant \log g \leqslant 4.5$. With a known iron abundance already derived from the Fe II absorption, the strength of the λ 6481 line therefore essentially indicates a program star's temperature, alone. The other Fe I lines measured display similar behavior, although the particular sensitivity of each to temperature varies, in detail, with the excitation potential of the line's lower level. Figure 3 shows that, for the example of the λ 6481 line, a typical observational error $\Delta W_\lambda \approx \pm 9$ mÅ can be expected to cause a random error $\Delta T_e \approx \pm 250$ K in the temperature inferred from this line, at $T_e \approx 5900$ K.

For each of the seven program stars, the observed equivalent widths of up to eight weak Fe I lines previously enumerated in Table I are given in Table IV; for comparison, the solar equivalent widths in integrated light taken from Table I are again tabulated as well. The particular Fe I lines measured were chosen in part because a very accurate experimental oscillator strength is available for each (Blackwell *et al.* 1982; 1986). No additional weak, unblended Fe I lines with comparably accurate oscillator strengths are detected reliably in our spectra of all seven cluster stars. The general range of temperatures in the cluster stars can now be anticipated immediately, from the equivalent widths alone. For any slightly hotter but solarlike star which also has a solar abundance of iron, Fig. 3 shows that the Fe I lines in the star's spectrum should be weaker than their respective solar counterparts, but by an amount which would not exceed the present observational uncertainty $\Delta W_\lambda(2\sigma) \approx \pm 9$ mÅ if the temperature excess is less than 250 K, for example. Any larger, detectable difference between the measured equivalent widths would therefore reveal a larger, real temperature difference between the star in question and the Sun. The average ratio of the 47 equivalent widths reported in Table III for the cluster stars, relative to their solar counterparts, is 0.88 ± 0.22, in fact; the effective temperature of a typical cluster turnoff star therefore is probably slightly hotter than solar, although an allowance for the marginally lower iron abundance in NGC 188 must also be made.

The quantitative effective temperatures derived from plots such as those in Fig. 3 are listed in Table IV, for each line and star. For this purpose, the previously determined average iron abundance $\log(Fe/H)_{cluster} = -4.65$ derived from all of the measured Fe II lines was assigned to each star individually. The value $\langle T_e \rangle$ calculated for each star by averaging the individual temperatures derived from the various lines is listed in the last column of the table.

In practice, a simple iterative procedure was actually used

TABLE IV. Fe I lines.

Star	6082.72 Å W_λ (mÅ)	6082.72 Å T_e (K)	6151.62 Å W_λ (mÅ)	6151.62 Å T_e (K)	6173.34 Å W_λ (mÅ)	6173.34 Å T_e (K)	6265.14 Å W_λ (mÅ)	6265.14 Å T_e (K)	6297.80 Å W_λ (mÅ)	6297.80 Å T_e (K)	6481.88 Å W_λ (mÅ)	6481.88 Å T_e (K)	6498.94 Å W_λ (mÅ)	6498.94 Å T_e (K)	6574.24 Å W_λ (mÅ)	6574.24 Å T_e (K)	$\langle T_e \rangle$ (K)
I-91	19	6180	51	5675	80	5395	99	5415	×	×	43	6170	53	5550	×	×	5730 ± 360
I-76	31	5795	×	×	46	6245	63	6250	×	×	46	6085	32	5955	20	5910	6040 ± 185
I-99	34	5705	49	5725	51	6115	68	6135	46	6425	74	5385	52	5560	21	5885	5865 ± 340
I-17	26	5940	56	5555	75	5510	×	×	84	5475	42	6195	46	5670	×	×	5725 ± 285
I-101	38	5600	44	5850	49	6175	64	6230	62	6025	62	5675	32	5955	22	5855	5920 ± 220
I-71	32	5765	40	5950	60	5885	×	×	51	6295	44	6145	31	5985	20	5910	5990 ± 175
I-49	30	5820	53	5620	47	6225	×	×	68	5875	45	6110	×	×	23	5830	5915 ± 220
Sun	33.6	5845	50.8	5785	73.9	5655	89.1	5730	73.8	5825	63.1	5755	43.9	5800	26.6	5825	5780 ± 65

to deduce the final values of both $[\mathrm{Fe/H}]_{\mathrm{cluster}}$ and the stellar temperatures. First, to determine the iron abundances from the Fe II lines, an initial trial value $T_e = 6000$ K was adopted for each star. The resulting average value of $(\mathrm{Fe/H})_{\mathrm{cluster}}$ was then used to ascertain the respective stellar values of $\langle T_e \rangle$ from the Fe I lines, as just described. These resulting individual temperatures were next used as improved starting estimates for a repetition of this whole analysis, first with the Fe II lines and then the Fe I lines. The iterative method converged rapidly for every star, never requiring more than three passes through both sets of lines.

For four of the seven stars, the standard deviation about their mean value $\langle T_e \rangle$ of the various temperatures deduced from the respective lines is $\sigma_T \leqslant 220$ K (Table IV), an amount smaller than the scatter of about ± 250 K which should arise merely from the random observational errors in measuring the equivalent widths. On the other hand, the largest temperature difference indicated between any two of the seven stars is $\Delta \langle T_e \rangle = 315$ K, a range slightly wider than this expected scatter. Furthermore, the correlation between the derived effective temperatures $\langle T_e \rangle$ and the observed $B-V$ colors, uncorrected for reddening, is surprisingly good, in view of the large random errors and the small range of the derived temperatures. The correlation is shown in the Appendix. This discussion suggests that actual differences in temperature exist among these seven turnoff stars, but that the random temperature errors resulting from the measurement of weak lines are comparable in magnitude to those real differences. In order to assign a single temperature which crudely characterizes the turnoff region in NGC 188, the average value $\langle T_e \rangle_{\mathrm{turnoff}} = 5885 \pm 120$ K of all seven stars can be noted. This standard deviation probably includes significant contributions not only from the uncertainties in the observed equivalent widths but also from a real dispersion in stellar temperatures.

In precisely the same way as for the cluster stars, the solar equivalent widths have been used to deduce values of $T_{e_\odot}$ from each of the eight solar Fe I lines, for the abundance $\log(\mathrm{Fe/H})_\odot = -4.53$ (Sec. II). The eight lines correctly yield an average solar temperature of $\langle T_e \rangle_\odot = 5780 \pm 65$ K (Table IV), in agreement with the observed value. This result was predetermined by the procedure of Sec. II and in fact assures that the temperature excesses of the cluster stars with respect to the Sun have been determined differentially with reference to the correct solar temperature. In short, this calculation redundantly verifies directly that the temperatures derived for the cluster stars should be free of any *systematic* error in the zero point of the temperature scale. This freedom from systematic errors will be of importance in Sec. IV. We also emphasize again that the cluster stars possess atmospheres which appear to be physically very similar to the Sun's.

IV. AN AGE ESTIMATE

The foregoing results can be summarized in the statements that the average metallicity of NGC 188 is $[\mathrm{Fe/H}]_{\mathrm{cluster}} = -0.12 \pm 0.16$ and that the average effective temperature of seven stars in the turnoff region is $\langle T_e \rangle_{\mathrm{turnoff}} = 5885 \pm 120$ K. The purely spectroscopic method so far used does not effectively require any estimates of the reddening and the distance of the cluster stars, with their important attendant uncertainties. Such photometry has been used only in estimating approximately the stellar surface gravities (Table II). The analysis is so insensitive to these gravities (Fig. 1), however, that our results are changed by amounts appreciably smaller than the final errors cited just above, when most other published estimates of the luminosities are used instead (cf. VandenBerg 1985).

When a cluster's metallicity is known, one criterion which can be used to estimate the age of the cluster from stellar evolutionary tracks is the maximum effective temperature of the stars in the turnoff region. Thus, the underlying purpose in determining the temperatures of our program stars is to deduce an age for NGC 188. An extensive set of new evolutionary tracks which are accurately normalized to the Sun have been very kindly provided by VandenBerg (1990) and will be used for this purpose. The relevant isochrones are shown in Figs. 4 and 5; the actual cluster metallicity derived, $[\mathrm{Fe/H}] = -0.12$, corresponds to $Z \approx 0.0128$, or fairly closely to the average of the two most similar heavy-element abundances included among the evolutionary models, $Z = Z_\odot = 0.0169$ and $Z = 0.010$. Two different methods of comparing the temperatures derived from our spectra with these theoretical isochrones will now be investigated.

a) Effective Temperatures Only

A portion of the color–magnitude diagram of NGC 188 is shown in Fig. 6. As is further evident from Fig. 7 in the Appendix, the three hottest, bluest program stars near $V = 15.0$, namely I-76, I-101, and I-71, together define rather well the highest temperature actually attained by cluster

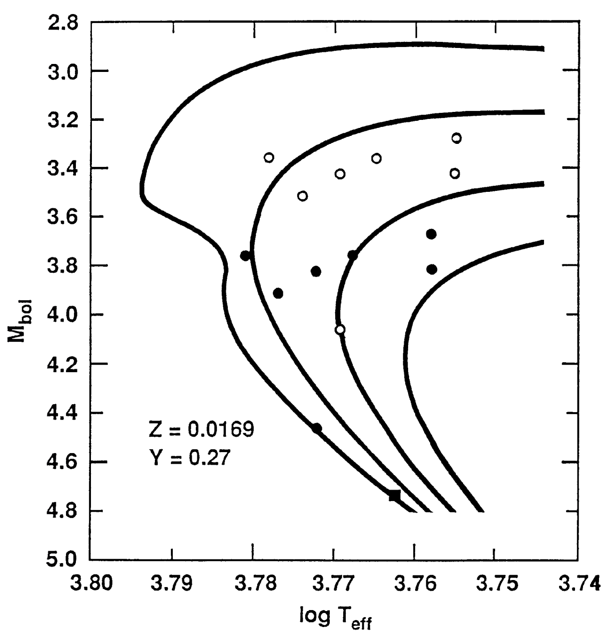

FIG. 4. The positions of the seven cluster stars in the theoretical H–R diagram (filled circles), with the absolute bolometric magnitudes of Table II. The open circles show bolometric magnitudes which are brighter by 0.4 mag. The consequent decreases in the inferred effective temperatures which are induced by the correspondingly lower surface gravities (Table II) are also taken into account. Also shown are four theoretical isochrones for ages of 4.5, 6, 8, and 10 Gyr, arranged from top to bottom, respectively, with $Y = 0.27$ and $Z = Z_\odot = 0.0169$ (VandenBerg 1990). The position of the Sun, to which the isochrones are precisely normalized, is shown by a filled square.

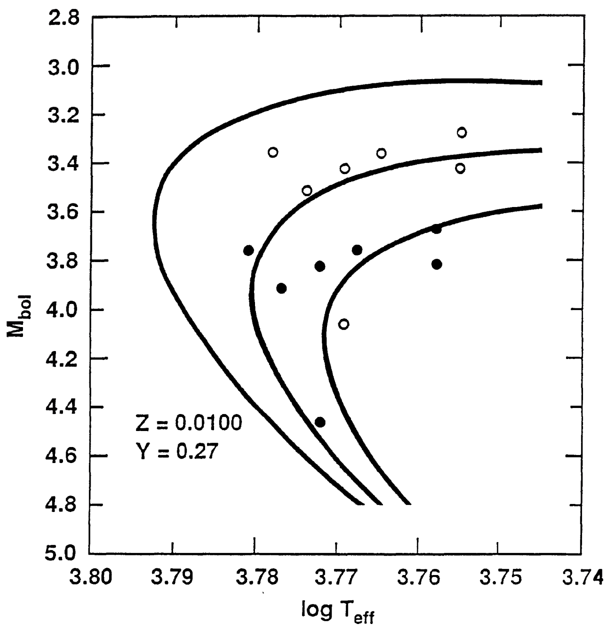

FIG. 5. Similar to Fig. 4, but for $Z = 0.0100$ and ages of 6, 8, and 10 Gyr. The position of the Sun is omitted.

stars in the turnoff region. From Table IV, the average of these three temperatures is $\langle T_e \rangle_{max} = 5980 \pm 50$ K, or log $\langle T_e \rangle_{max} = 3.777 \pm 0.004$. This empirical limiting temperature can be used immediately to estimate the cluster's age from the isochrones for each of the two metallicities. For $Z = 0.0169$ and 0.0100, the results are 6.6 and 8.8 Gyr, respectively; the relevant average value, which corresponds satisfactorily to $[Fe/H] = -0.12$, is $\tau = 7.7$ Gyr. The uncertainty of ± 0.004 in log $\langle T_e \rangle$ leads to a 2σ uncertainty of about ± 1.4 Gyr, from both sets of isochrones. Our preferred estimate of the age of NGC 188 therefore is $\tau = 7.7 \pm 1.4$ Gyr. Owing to the relatively slow pace of nuclear burning in these stars of low mass, the age inferred in such a way depends very sensitively upon T_e, no matter what method is used to determine the latter. Our temperatures, which have been derived differentially with respect to the Sun for these solarlike stars and are effectively independent of the reddening and the distance adopted for the cluster, should be free of crucial *systematic* errors, despite the relatively large random observational errors introduced by our analysis of weak lines.

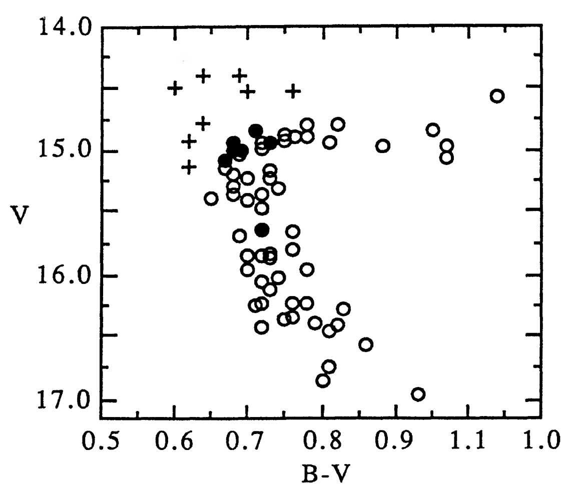

FIG. 6. A portion of the color–magnitude diagram of NGC 188 near the turnoff (ES). The seven program stars are shown as filled circles, and eight stars identified by ES as blue stragglers are shown as crosses.

Our estimate of the age of NGC 188 is intermediate between the younger values between 5 and 6.5 Gyr determined by Demarque and McClure (1977), Twarog and Anthony-Twarog (1989), and Caputo *et al.* (1990), on the one hand, and the older ones near 10 Gyr estimated by Iben (1967) and VandenBerg (1985) on the other hand. All of the earlier values were based upon the observed colors, not the spectra, of the cluster stars, and a major contribution to the resulting discrepancies among those ages therefore arose from the different respective assumptions made about the reddening and the distance of the cluster, parameters to which our analysis is quite insensitive.

b) The H–R Diagram

The method just used takes advantage of the available data for only three of the seven program stars. It also provides no check on the consistency of the inferred luminosities of the cluster stars with the theoretical values available from the evolutionary tracks. Therefore, the seven program stars have also been plotted along with the isochrones, in the theoretical H–R diagrams of Figs. 4 and 5. The required bolometric magnitudes are taken from Table II, and the effective temperatures again are those determined from the Fe I lines and given in the last column of Table IV. If the masses derived from the evolutionary tracks for the respective metallicities of Figs. 4 and 5 are averaged, the theoretical stellar masses of the program stars range from about $1.0\mathcal{M}_\odot$ for star I-49, near the ZAMS, to about $1.1\mathcal{M}_\odot$ for several of the stars which have evolved farther from the ZAMS.

The average age is then deduced by estimating ages for the stars individually from the isochrones in the full H–R diagram. The result is readily found to be $\langle \tau_1 \rangle = 8.5 \pm 1.4$ Gyr, when star I-49 near the ZAMS is excluded because of the relatively large uncertainty in its inferred age. This age estimate is similar to the one derived previously, and more reliably, from the limiting turnoff temperature alone. The qualitative agreement between the stellar data and any one isochrone interpolated for $Z \approx 0.0128$ (not shown) also is not inconsistent with our estimates of the random errors expected in the spectrsocopic temperatures. In contrast to the age derived from the maximum temperature alone, however, this result does depend significantly upon the assumed reddening and distance of the cluster (Table II), because these parameters govern the luminosities deduced for the stars. In order to explore this dependence briefly, the values of M_{bol} in Table II can be arbitrarily varied by ± 0.4 mag, an amount which appears to limit the plausible range.

For bolometric magnitudes brigher by this amount, the positions of the stars are replotted in Figs. 4 and 5 as open circles. The age now determined by the identical procedure is $\langle \tau_2 \rangle = 7.1 \pm 0.5$ Gyr, a value which overlaps substantially the preferred one, $\tau = 7.7 \pm 1.4$ Gyr, but only at the young end of that range. A more important feature of the higher luminosities perhaps is the reduced dispersion among the individual ages; the better agreement of the stellar data with a particular isochrone is evident in each of Figs. 4 and 5, and also persists for the isochrones interpolated for $Z \approx 0.0128$. This intrinsically less reliable method therefore favors both an age nearer 7 Gyr and bolometric magnitudes approximately 0.4 mag brigher than those in Table II, and hence a correspondingly larger cluster reddening and/or distance modulus.

The implausibility of bolometric magnitudes brighter than those in Table II by more than 0.4 mag derives from the observed absence, with one exception, of turnoff stars which are hotter than our hottest program stars. For ages of about 6 Gyr and younger, the isochrones interpolated for $Z \approx 0.0128$ require the presence of a number of hotter stars, which apparently do not actually exist in the color–magnitude diagram of NGC 188 (Fig. 6). The putative absence of a zero-point error in our spectroscopically determined temperatures is to be underlined once again. The complementary implausibility of bolometric magnitudes fainter than those in Table II by even 0.4 mag derives from the resulting much poorer fit of the data for the cluster stars to any one isochrone for either metallicity, or for $Z \approx 0.0128$. For the latter metallicity, the individually deduced ages span the unacceptably wide range from about 4 to 12 Gyr, and star I-49 lies well below the ZAMS.

V. SUMMARY AND DISCUSSION

Apparently for the first time, the classical combination of high-resolution spectra and model stellar atmospheres has been applied to seven generally solarlike, turnoff stars in NGC 188. This method of deducing directly the metallicity and the effective temperatures of the cluster stars yields $[\mathrm{Fe/H}]_{\mathrm{cluster}} = -0.12 \pm 0.16$ and $\langle T_e \rangle_{\mathrm{turnoff}} = 5885 \pm 120$ K. A turnoff age $\tau \approx 7.7 \pm 1.4$ Gyr is then derived by comparing the deduced upper limit on the turnoff temperatures with the appropriate isochrones in the theoretical H–R diagram. All of these conclusions are effectively independent of the values assumed for the reddening, the intrinsic colors, and the distances of the cluster stars, with their associated uncertainties. A similar, auxiliary investigation of the luminosities of the cluster stars in the H–R diagram favors the young end of the cited range of ages, but it is less intrinsically reliable owing to its sensitivity to possible errors in the assumed cluster parameters.

An additional potential uncertainty in our age estimate (only) has been alluded to throughout this work by referring specifically to the cluster's "turnoff age." Because our observations have been confined to solarlike stars, the conclusions derived from the model atmospheres should be especially reliable. A disadvantage of this constraint, however, is that the data refer to only an extremely limited region of the cluster's H–R diagram, near the turnoff, as is partially indicated in Fig. 6. Twarog and Anthony-Twarog (1989) and Caputo *et al.* (1990) have argued that significant discrepancies exist between the morphology of the color–magnitude diagram of NGC 188 and that of the older theoretical isochrones of VandenBerg (1985), after the latter are transformed to the observational diagram or vice versa. Such a conclusion is of course affected by all of the well-known difficulties which arise in this transformation. More importantly, a similar comparison has not yet been carried out for the new isochrones used exclusively here. The resolution of any such discrepancy, if one were to be clearly established in the future, is outside the scope of this paper and presumably involves fundamental matters, such as mass loss, opacities, or the mixing-length approximation (Pedersen, VandenBerg, and Irwin 1990). While our effective temperatures for the turnoff stars in NGC 188 should be quite dependably determined, the turnoff age deduced from those temperatures obviously depends sensitively on any such errors in any set of evolutionary tracks adopted. Our formal age uncertainties necessarily are lower limits which cannot include such unknown effects.

Finally, one additional potential source of error in our results should be addressed. A microturbulent velocity $v_t = 1$ km s^{-1} has been uniformly used in interpreting the cluster spectra. This nearly solar value was adopted because the accuracy of our equivalent widths is too poor to allow us to derive v_t from the spectra (cf. BSS). Since the cluster stars are found to be significantly older than the Sun, it is possible that some smaller value $v_t < 1$ km s^{-1} is more nearly correct, if v_t declines with increasing age. Although relatively weak lines were analyzed precisely in order to minimize the effects of this uncertainty on our conclusions, it is important to test the magnitude of these dependencies. The entire analysis presented above has therefore been repeated for $v_t = 0.5$ km s^{-1}, a choice which leads to an estimate of slightly greater saturation of the lines. The corresponding results are $[\mathrm{Fe/H}] = -0.01 \pm 0.15$ and $\langle T_e \rangle_{\mathrm{turnoff}} = 5910 \pm 130$ K; each value lies well within the respective error range already determined for $v_t = 1$ km s^{-1}. Owing primarily to the effects of the higher metallicity, the corresponding age $\tau = 6.3$ Gyr derived as above is appreciably younger but lies just within the previously determined range of uncertainty. Thus, our imprecise knowledge of v_t for the turnoff stars in NGC 188 does not appear to affect significantly our previous conclusions derived from weak spectral lines.

It is a pleasure to acknowledge the help of Caty Pilachowski, who critically read the manuscript and made numerous useful suggestions. We are also very grateful to Don VandenBerg for entirely similar help and especially for providing us with his new isochrones in advance of their publication. In addition, Dimitri Mihalas provided valued advice about the method of analysis. David Lambert, Earl Luck, and Ruth Peterson gave us guidance in ascertaining oscillator strengths and solar equivalent widths. Financial support was provided for this work by the National Science Foundation, through Grant Nos. AST-8614218 and AST-8820894 to the University of Chicago.

APPENDIX

The metallicity and the temperatures derived above for the cluster stars can be used together to estimate the intrinsic $B-V$ colors of the stars. These intrinsic colors can then be compared with the observed colors, to derive the interstellar reddening of the cluster. For completeness, such an analysis is carried out. It has been relegated to this Appendix, however, in the hope of improved logical clarity, because the spectroscopic method used above essentially avoids the use of these color indices.

Specifically, in order to calculate $(B-V)_0$ for each program star, the calibration $T_e = 8065 - (3580 \times (B-V)_0(1-0.196[\mathrm{Fe/H}]))$ of Saxner and Hammar-

TABLE V. The reddening of NGC 188.

Star	T_e (K)	$(B-V)_0$	$B-V$	$E(B-V)$
I-91	5730	0.64	0.71	0.07
I-76	6040	0.55	0.68	0.13
I-99	5865	0.60	0.73	0.13
I-17	5725	0.64	0.69	0.05
I-101	5920	0.59	0.68	0.09
I-71	5990	0.57	0.67	0.10
I-49	5915	0.59	0.72	0.13

back (1985) is adopted, with [Fe/H] $= -0.12$ and the temperatures listed in Table IV above. The results are given in column 3 of Table V. The $(B-V)$ color indices measured by ES are given in column 4 of Table V, and their correlation with the spectroscopically determined temperatures listed in column 2 is additionally shown in Fig. 7. The resulting color excesses $E(B-V)$ appear in the last column. The average of these seven values is $\langle E(B-V) \rangle = 0.10 \pm 0.03$. This result is consistent with most published estimates of the reddening of NGC 188 but lacks sufficient precision to distinguish reliably among them.

Note added in proof: Dr. Pierre Demarque very kindly has sent us copies of new Yale evolutionary isochrones calculated for solar composition. These results are to be published shortly by P. Demarque, E. M. Green, and D. B. Guenther. At least within the generally circumsolar region of the H–R diagram shown here in Fig. 4, the new VandenBerg isochrones and the new Yale isochrones are very similar. This favorable comparison is to be expected, because both sets of models are normalized accurately to the Sun. We estimate the ages τ, τ_1, and τ_2 deduced here for NGC 188 from the VandenBerg models would be changed by less than ± 0.2 Gyr, depending on the particular opacity mixture chosen, had we used the new Yale models instead.

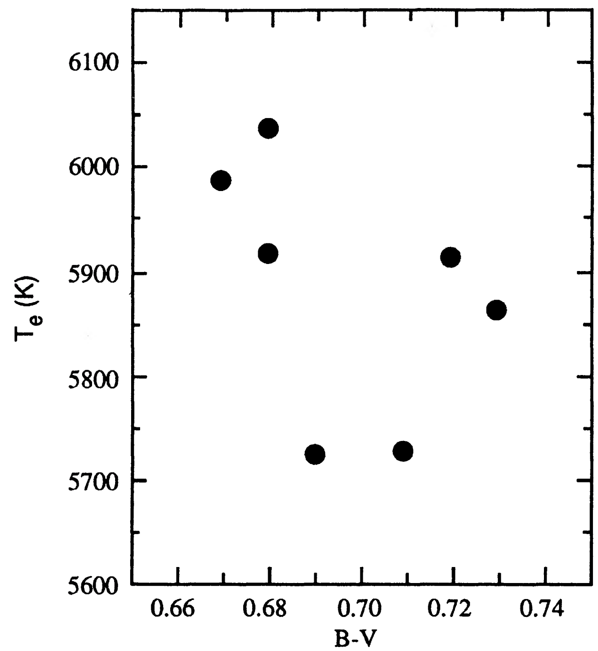

FIG. 7. The relation between the spectroscopically derived effective temperatures (Table IV) and the $B-V$ colors measured by ES, uncorrected for reddening, for seven turnoff stars in NGC 188.

REFERENCES

Blackwell, D. E., Booth, A. J., Haddock, D. J., Petford, A. D., and Leggett, S.K. (1986). Mon. Not. R. Astron. Soc. **220**, 549.

Blackwell, D. E., Petford, A. D., Shallis, M. J., and Simmons, G. J. (1982). Mon. Not. R. Astron. Soc. **199**, 43.

Blackwell, D. E., Shallis, M. J., and Simmons, G. J. (1980). Astron. Astrophys. **81**, 340 (BSS).

Caputo, F., Chieffi, A., Castellani, V., Collados, M., Martinez Roger, C., and Paez, E. (1990). Astron. J. **99**, 261.

Code, A. D., Davis, J., Bless, R. C., and Brown, R. H. (1976). Astrophys. J. **203**, 417.

Demarque, P., and McClure, R. (1977). In *The Evolution of Galaxies and Stellar Populations,* edited by B. M. Tinsley and R. B. Larson (Yale University Observatory, New Haven).

Eggen, O. J., and Sandage, A. (1969). Astrophys. J. **158**, 669 (ES).

Hobbs, L. M., and Pilachowski, C. (1988). Astophys. J. **334**, 734.

Iben, I. (1967). Astrophys. J. **147**, 624.

Kurucz, R. L. (1979). Astrophys. J. Suppl. **40**, 1.

Kurucz, R. L., Furenlid, I., Brault, J., and Testerman, L. (1984). *Solar Flux Atlas from 296 to 1300 nm* (National Solar Observatory Atlas No. 1).

Larson, R. B. (1990). Publ. Astron. Soc. Pac. (in press).

Pedersen, B. B., VandenBerg, D. A., and Irwin, A. W. (1990). Astrophys. J. **352**, 279.

Rutten, R. J., and van der Zalm, E. B. J. (1984). Astron. Astrophys. Suppl. **55**, 171.

Saxner, M., and Hammarback, G. (1985). Astron. Astrophys. **151**, 372.

Trimble, V., and Bell, R. A. (1981). Q. J. R. Astron. Soc. **22**, 361.

Twarog, B. A., and Anthony-Twarog, B. J. (1989). Astron. J. **97**, 759.

Upgren, A., Mesrobian, W. S., and Kerridge, S. J. (1972). Astron J. **77**, 74.

VandenBerg, D. A. (1985). Astrophys J. Suppl. **58**, 711.

VandenBerg, D. A. (1990). In preparation.

Wheeler, J. C., Sneden, C., and Truran, J. W. (1989). Annu. Rev. Astron. Astrophys. **27**, 279.